AGE (2012) 34:27–41
DOI 10.1007/s11357-011-9211-y

Sequential stages in the age-dependent gradual formation and accumulation of tubular aggregates in fast twitch muscle fibers: SERCA and calsequestrin involvement

Simona Boncompagni · Feliciano Protasi · Clara Franzini-Armstrong

Received: 1 September 2010 / Accepted: 24 January 2011 / Published online: 12 February 2011

Abstract Tubular aggregates (TAs), ordered arrays of elongated sarcoplasmic reticulum (SR) tubules, are present in skeletal muscle from patients with myopathies and are also experimentally induced by extreme anoxia. In wild-type mice TAs develop in a clear age-, sex- (male), and fiber type- (fast twitch) dependence. However, the events preceding the appearance of TAs have not been explored. We investigated the sequential stages leading to the initial appearance and maturation of TAs in EDL from male mice. TAs' formation requires two temporally distinct steps that operate via different mechanisms. Initially (before 1 year of age), the SR Ca^{2+} binding protein calsequestrin (CASQ) accumulates specifically at the I band level causing swelling of free SR cisternae. In the second stage, the enlarged SR sacs at the I band level extend into multiple, longitudinally oriented tubules with a full complement of sarco(endo)plasmic reticulum Ca^{2+} ATPases (SERCA) in the membrane and CASQ in the lumen. Tubules gradually acquire a regular cylindrical shape and uniform size apparently in concert with partial crystallization of SERCA. Multiple, small TAs associate to form fewer mature TAs of very large size. Interestingly, in fibers from CASQ1-knockout mice abnormal aggregates of SR tubules have different conformation and never develop into ordered aggregates of straight cylinders, possibly due to lack of CASQ accumulation. We conclude that TAs do not arise abruptly but are the final result of a gradually changing SR architecture and we suggest that the crystalline ATPase within the aggregates may be inactive.

Keywords Tubular aggregates · Sarcoplasmic reticulum · Calsequestrin · EDL · Electron microscopy

Abbreviations

TAs	Tubular aggregates
CRUs	Calcium release units
EM	Electron microscopy
CASQ	Calsequestrin
SR	Sarcoplasmic reticulum
jSR	Junctional SR
TT	T-tubule transverse tubule
SERCAs	Sarco(endo)plasmic reticulum Ca^{2+} ATPases

S. Boncompagni · F. Protasi
IIM—Interuniversitary Institute of Myology,
DNI—Department of Neuroscience and Imaging,
CeSI—Centro Scienze dell'Invecchiamento,
Università degli Studi G. d'Annunzio,
66013 Chieti, Italy

S. Boncompagni · C. Franzini-Armstrong
Department of Cell and Developmental Biology,
University of Pennsylvania,
Philadelphia, PA 19104-6058, USA

S. Boncompagni (✉)
CeSI, Center of Research on Aging,
Università G. d'Annunzio of Chieti,
Chieti, CH 66013, Italy
e-mail: s.boncompagni@unich.it

DHPR	Dihydropyridine receptor
RYRs	Ryanodine receptors
WT	Wild type
CM	Confocal microscopy

Introduction

The sarcoplasmic reticulum (SR) is a complex system of cisternae and tubules specific to muscle cells, which functions as an intracellular store for calcium (Ca^{2+}). The SR membranes act as a boundary controlling Ca^{2+} release, re-uptake.and storage. The SR accomplishes these critical tasks using specific proteins: luminal calsequestrin (CASQ) to increase capacity for Ca^{2+} storage ryanodine receptors (RYRs) to release Ca^{2+}; and the sarco(endo)plasmic reticulum Ca^{2+} ATPase (SERCA) for Ca^{2+} reuptake. An unusual accumulation of elongated SR-derived tubules, defined *tubular aggregates* (TAs) occurs in a variety of muscle conditions. TAs were first described as proliferations of the SR in a human myopathy (Engel 1964; Engel et al. 1970) and found to be a relatively nonspecific alteration in patients with various neuromuscular disorders including, but not limited to, periodic paralysis, some types of congenital myasthenic syndromes, and myotonic disorders (Rosenberg et al. 1985; Pierobon-Bormioli et al. 1985; Morgan-Hughes 1998). Since the human and animal diseases that present these morphological alterations are quite varied, and TAs are sometimes also found in asymptomatic probands (Niakan et al. 1985; Engel et al. 1970; Muller et al. 2001), the relationship of TAs to disease and/or particular physiological states is still debated. In animal models, TAs have been not only been associated to extreme hypoxia in rats (Schiaffino et al. 1977) but also described in mice carrying apparently unrelated mutations, such as dystrophin-null (Craig and Allen 1980) and Caveolin-1 and -2 deficient mice (Schubert et al. 2007). The possible participation of mitochondria in TAs' formation is not confirmed (Engel 1964; Novotova et al. 2002; Vielhaber et al. 2001). Indeed mitochondrial markers are restricted to the periphery of TAs in human muscle (Chevessier et al. 2005).

With the exception of sarcopenia and a general decrease in CRUs (Boncompagni et al. 2006; D'Incecco et al. 2010), skeletal muscle fibers show few structural changes that are specifically related to aging. For that reason, TAs have attracted considerable attention because they seemed an aging phenomenon in mouse muscles, although limited almost exclusively to fast-twitch skeletal muscle fibers of males from inbred strains (Agbulut et al. 2000; Chevessier et al. 2004). Interestingly, females are excluded and the difference seems to be under hormonal control (Yoshitoshi et al. 1991).

The derivation of TAs from the SR was confirmed by demonstrating their content of SERCA and CASQ (Salviati et al. 1985; Chevessier et al. 2004). The term TA has also been extended to other SR accumulations with variable appearances (Pavlovicova et al. 2003 for a review), but here, we will restrict the term to densely packed aggregates of straight tubular membranes with SR origin and that contain amorphous electron-dense material.

Very little is known regarding the events leading to TAs' formation, and the function of these unusual structures is still unclear. In order to explore the timing, formation, and potential role of TAs in skeletal muscle, we examined muscle fibers at different ages (2 to 29 months) in male and female inbred mice (C57Bl/6) and in a CASQ null mouse model. Our work confirms past observations that TAs' formation is age, fiber type, and sex dependent. We find that TAs' formation, a phenomenon thought to be a specific sign of aging in fast skeletal muscle fibers, follows a progression of events that start as minor structural alterations at an early age (3 to 4 months) but become dramatically evident, with the accumulation of large tubular aggregates only at older ages. Two separate but sequential stages in TA formation are marked by and perhaps driven by an initial accumulation of CASQ1 followed by a subsequent increase in both CASQ1 and SERCA. The latter protein acquires an inactive configuration. Based on these results, we suggest a novel interpretation of TAs presence, and we provide a fuller understanding of the critical processes and contributing proteins in this age-related specific phenomenon.

Materials and methods

Electron microscope identification of fiber types in the EDL. Fiber types are mostly classified on the basis of myosin heavy chain isoform expression and myosin ATPase activity. EDL contains ~70–75% type IIB,

~10–15% type IIX, ~8% type IIA, and ~4% type I (Danieli-Betto et al. 2005; Augusto et al. 2004; Hughes et al. 1999). The reported percentages of the IIX–IIB fibers in EDL are somewhat variable, in part because immunolabeling alone does not always give a clear distinction and in part because the ratios of the two fibers vary in different regions of the muscle and/or in different mouse lines. In general, the oxidative capacity of the fast fibers increases in the order: IIA>IIX>IIB. Based on the fact that these three types of fast fibers have different content and disposition of mitochondria and different size and shape, we used cross sections for electron microscopy (EM) to discriminate among them, as follows: (1) type IIB fibers have mitochondria positioned exclusively at the level of the I band; (2) type IIX fibers have a majority of mitochondria not only at the I band level but also few at the A band and occasionally in small subsarcolemmal clusters; (3) type IIA fibers are clearly different, having a smaller diameter and frequent mitochondria at both A and I band levels and in large clusters at the fibers' edges; (4) Type I fibers are very rare, confined in a region of the muscle that was not embedded and, thus, were not encountered in this study.

Embedding and thin sectioning for EM. C57Bl/6 wild-type (WT) and CASQ1-null mice between 2 and 29 months of age were killed by cervical dislocation. EDL muscles were dissected, pinned to a Sylgard dish (Dow Corning) at resting length; fixed with 3.5% glutaraldehyde in 0.1 M sodium cacodylate buffer (pH 7.2) at room temperature (RT); and then stored in fixative at 4°C for variable periods of time. Muscle segments were post-fixed in 2% OsO_4 in the same buffer for 1–2 h at 4°C, en block-stained in saturated uranyl acetate and embedded in Epon 812. Ultrathin sections (about 40 nm) were cut in an ultramicrotome Leica Ultracut R (Leica Microsystem, Austria) using a Diatome diamond knife (DiatomeLtd. CH-2501 Biel, Switzerland) and stained in 4% uranyl acetate and with lead citrate solutions.

Crude SR fraction preparation. EDL muscles from an aging mouse (17 months) were finely minced in 5 mM EGTA, 10 mM DL-histidine, in 0.25 M sucrose with a protease inhibitor cocktail (Roche Diagnostics GmbH, Mannheim, Germany), and 0.1 mM of leupeptin and homogenized in a Tekmar Tissumizer (Tekmar Cop., Cincinnati, Ohio) three to four times at maximum speed for 2 s. The homogenate was centrifuged at 18,000×*g* for 30 s at RT, and the supernatant was centrifuged again at 18,000×*g* for 10 min in an Eppendorf microfuge (4°C). The pellet was resuspended in a small volume of the same solution and used immediately for rotary shadowing.

Freeze-fracture (FF) and rotary shadowing. Muscle specimens for FF were fixed as described above (previous section). Small bundles of fixed fibers were cryoprotected in 30% glycerol, mounted between two copper holders covered with a thin layer of 20% polyvinyl alcohol in 30% glycerol and frozen in liquid nitrogen-cooled propane. The bundles were then freeze-fractured under vacuum, shadowed with platinum at 45° and replicated with carbon in a Blazer's 400 freeze fracture unit (Balzers, model BFA 400; Balzers S.p.A., Milan, Italy). Crude SR fraction were freeze-dried, rotary shadowed, and replicated as in Ferguson et al. (1985).

Sections and FF replicas were examined either in a FP 505 Morgagni Series 268D electron microscope (Philips, Hamburg, Germany) at 60 kV equipped with Megaview III digital camera and Soft Imaging System (Munster, Germany) or in a Phillips 410 electron microscope (Philips Electron Optics, Mahwak, NJ) equipped with a Hamamatsu C4742-95 digital imaging system (Advanced Microscopy Techniques, Chazy, NY).

Immunofluorescent labeling for CM. For confocal microscopy (CM), dissected EDL muscles from WT mice (17 months of age) were fixed in 2% paraformaldehyde in phosphate-buffered saline (PBS) for 20 min at RT. Smalls bundles of fibers were blocked for 1 h in PBS containing 1% bovine serum albumin (BSA), 10% goat serum, and 0.5% TRITON X-100 and then incubated overnight at 4°C with primary antibodies. After wash in PBS/BSA (3×15 min), fibers were incubated in for 1 h at RT in secondary antibodies (CY3-conjugated and goat anti-rabbit, Jackson Immuno-Research Laboratories, Lexington, KY, USA), washed again, and finally mounted with an anti-bleach medium (glycerol containing 0.0025% para-phenylenediamine, 0.25% 1,4 diazobicyclo-2,2,2-octane, and 5% *N*-propylgallate). Specimens were observed in a scanning confocal microscope equipped with Ar–Kr laser (LS510 META, Carl Zeiss, Germany).

The following primary antibodies were used: 34 C, mouse monoclonal, diluted 1:30 (Airey et al. 1990; purchased from Developmental Studies Hybridoma Bank, University of Iowa), which recognizes both RYR1 and RYR3 isoforms; 4B1.D3, mouse monoclonal anti-CASQ, diluted 1:400 (Jones et al. 1998), which specifically recognizes the CASQ1 isoform. The 4B1.D3 antibody was a generous gift of L. A. Jones (Indiana University).

Count of free SR tubule profiles. The relative frequency of free SR tubule profiles of different sizes was performed in random photographs from cross sections, taken at magnification of ×84.400 (see Tables). Classification of profile was based on an approximate size estimate. A circle up to ~70 nm of diameter covered the smallest profiles: ~80–150, 150–200, and >200 nm identified medium, large, and extra large profiles, respectively.

Preparation of figures. Figures were mounted and labeled using Adobe Photoshop® v7.0.

Results

The configuration of the free SR domain at the I band level in type IIX and IIB fibers of male mice changes in an age dependent manner. The SR of adult mammalian muscle is comprised of two domains (Fig. 1a): the junctional SR (jSR) constituting the two lateral sacs of the triad, containing CASQ in its lumen and forming triads with T-tubules (TT); and the free SR also called longitudinal SR, that extends on both sides of the triad, along the entire sarcomere. The free SR differs from the jSR because it has CASQ in its lumen and a high concentration of Ca^{2+} pump (SERCA) in its membrane. Due to the position of triads at the level of the A–I junction, the free SR of mammalian muscle is further divided into two segments positioned beside the A band (Fig. 1a, white arrows) and the I-Z-I regions of the sarcomere (Fig. 1a, empty arrow). The two segments are not morphologically identical: the I band free SR is composed mostly of irregular and convoluted tubules and it often occupies two or three layers between the myofibrils (Fig. 1b, arrows); the A band free SR is a combination of tubules and flat fenestrated cisternae, and it is almost exclusively constituted of a single layer between the myofibrils (Fig. 1a, white arrows). This difference is likely due to space constrains, since the intermyofibrillar spaces are wider at the I-Z-I level.

The first noticeable change of the SR, which starts to develop quite early, occurs specifically in IIB and IIX fibers of males: the sectioned profiles of both junctional and free SR at the I band level, appear dilated (Fig. 1c and d, empty arrows). Although the dilation becomes gradually more prominent, it never affects the free SR at the A band level. Initially, the smaller SR profiles appear empty, but the wider ones contain an electron-dense matrix (see detail in Fig. 1d). We identify the SR luminal content as CASQ based on two observations: first, its appearance is identical to that found in the jSR, whose luminal content is well established to be CASQ (Meissner et al. 1973; Campbell et al. 1980); secondly, and more directly relevant to this work, in CASQ1-null EDL fibers the I band SR never shows any dilation (Fig. 1e and f) and does not display such a dense content (detail in Fig. 1f).

The progression of changes can be traced quantitatively by classifying the profiles of free SR tubules seen in cross sections at the level of the I band into four categories (Table 1). The first category (small) includes small circular profiles, up to ~70 nm in diameter (Fig. 1b). Profiles in the other three categories have size ranges of ~80–150 nm (medium profile, Fig. 1d enlarged detail, white arrows); 150–200 nm (large profile, Fig. 1c and d, empty arrows); and >200 nm (extra-large profile) in diameter (not shown). Larger SR tubules are more variable in size and shape than the original smaller tubules (Fig. 1b). Very few SR tubules are dilated at 2 to 3 months, but an increasing number are noticeably larger at 7 months and a higher percentage of tubules are very enlarged between 12 and 24–27 months (Table 1). In parallel to the SR enlargement, there is also a gradual decline in the frequency of the sectioned SR profiles (a ~40% reduction between 2 and 12 months of age, Table 2, column E). Importantly, dilated SR tubules are almost totally absent in muscles from females even at late ages (Table 1).

The change in shape of the I band SR occurs with a very small increase in overall volume and a small decrease in surface area. Morphometric analysis shows approximately 10% and 20% increase in I

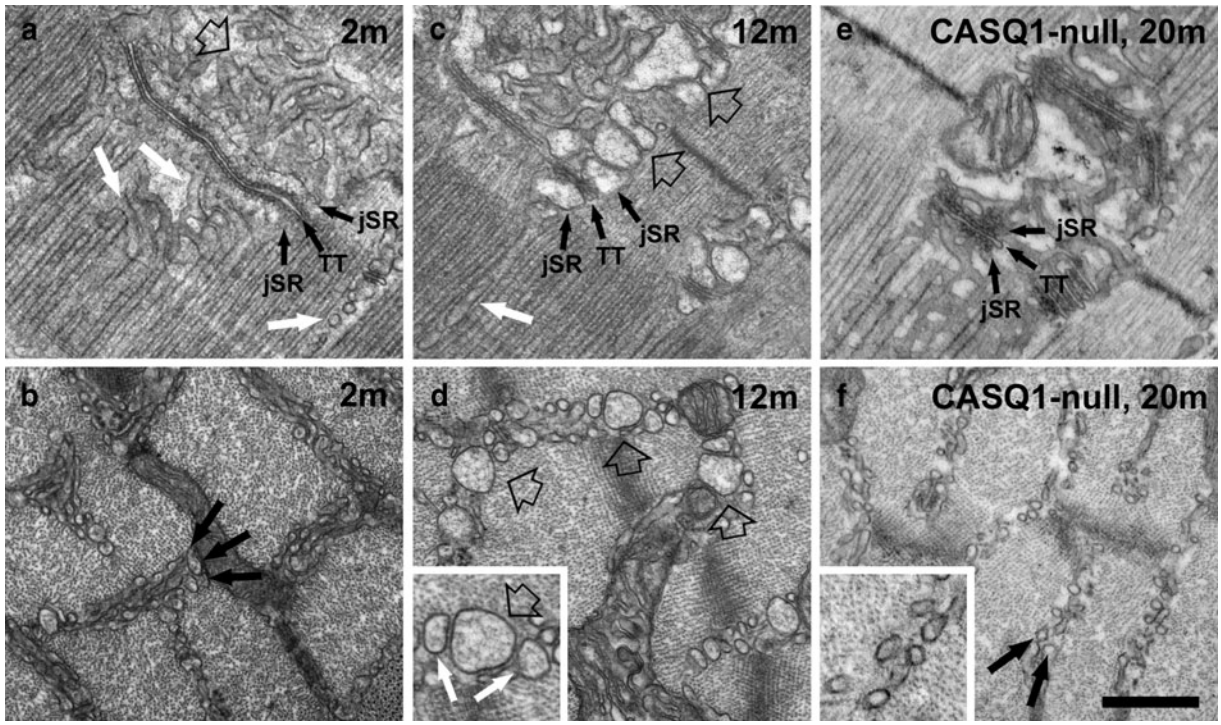

Fig. 1 The Initial step in the formation of TAs is the remodeling of the SR at the I band in IIB/IIX fibers of male mice. **a** and **b** SR is constituted of jSR (labeled), forming triads with T-tubules (TT) and free SR, composed of narrow, meandering tubules (**a**, *empty and white arrow*). At the I band level (**b**, *black arrows*) the free SR is arranged in two to three layers. At 2 to 3 months of age (**a**, **b**) the I band free SR has small, mostly empty profiles. **c**, **d** At 12 months, both jSR (labeled) and free-SR-sectioned profiles at the I band are often wider and have a visible electron dense content (*empty arrows*). Dilation of the free SR does not occur at the A band level (**c**, *white arrow*). The enlarged detail in **d** shows medium (*white arrows*) and large (*empty arrow*) SR profiles. **e**, **f** In CASQ1-null EDL fibers, the jSR cisternae (labeled) are reduced in size compared to WT. Neither jSR nor free SR change size and shape with increasing age in absence of CASQ1 (**f**, *arrows*). *jSR* junctional SR; *TT* transverse tubules. *Bar* 0.5 μm

band SR volume at 7–8 and 12 months, respectively, relative to 2 to 3 months, whereas the surface area marginally decreases during this period (Table 2). The increase in the cross-sectional areas of individual tubules, with only a minor change in the surface area and volume of the whole SR segment, indicates that there is a rearrangement of the SR shape.

Formation and maturation of tubular aggregates is a further change in older male mice. In Type IIB–IIX fibers of older male mice (>15 months), the dilated free SR cisternae often coexist with aggregates of longitudinally oriented elongated SR-derived tubules that invade both A and I bands (Fig. 2). The elongated tubules (Fig. 2, stars) are directly continuous with the dilated I band level SR cisternae (Fig. 2a, empty arrows) and indeed seem to be directly derived from them. The electron dense content of the dilated I band SR, i.e., CASQ, continues without either interruptions or change in appearance into the lumen of the elongated tubule, indicating that CASQ expand from the junctional SR into dilated free SR vesicles at the I band and into nascent longitudinal tubules where it is normally not found. Tubules in process of elongation displace triads and the longitudinal SR network over the A band and gradually aggregate into bundles, the nascent TAs (Fig. 2a and c) that increase in size and frequency with age.

Two variations of SR shapes are present in TAs of all sizes, and these are illustrated in cross sections of the bundles. Dilated SR tubules of variable shapes are located at the very edges of smaller and larger TAs (Fig. 2b, empty arrows); closer to the center, the tubules have a circular cross section, and they are quite uniform in diameter. Longitudinal sections and freeze-fracture replicas confirm that the more central-

Table 1 Size and frequency of sectioned SR profiles in the I band of type IIX–IIB fibers

Age	Sex	A Small (~30–70 nm) profiles% of total	B Medium (~80–150 nm) profiles% of total	C Large (~150–200 nm) profiles% of total	D X-Large (> 200 nm) profiles% of total	E No. of SR profiles/area (μm^2)
2–3 months	Male	98±2	2±2	0	0	29±8
7–8 months	Male	90±9	9±9	1±1	0	22±4
12 months	Male	89±10	9±8	2±5	0	17±6
24–27 months	Male	73±17	22±14	7±6	0.28±1	N/A
12–29 months	Female	96±4	4±4	0	0	N/A

Mean±SD. All data for males are from 31 fibers each in three mice. For females, 20 fibers each for three mice; Student's *t* test: 2–3 vs 7–8 months: $P<0.001$ for small and medium and large profile; 7–8 vs 12 months: no significantly different; 12 vs 24–27 months: $P<0.00001$ for small, medium, and large profile

ly located tubules are cylindrical (Fig. 2a and c, see also Fig. 3), whereas the peripheral ones are more variable in shape (Fig. 2b and d). Based on the size and center-to-center distances of tubules, we calculate that the approximate surface and volume densities of SR tubules within the cores of TAs are extremely high: 31.3 and 0.52 $\mu m^3/\mu m^3$ (Table 2).

Myofibrils are excluded from small and large TA regions, so that cross striations end abruptly at their edges. It is noticeable that within the rest of the fiber and also immediately adjacent to TAs, both myofibrils and A-band SR have a normal structure: there is no evidence of decay or damage to the overall contractile architecture.

Very large aggregates are formed by association of multiple smaller TAs. Multiple TAs of variable size initially appear in cross sections of IIB–IIX fibers from EDL at ~15 months of age, but at later ages only 1 or 2, much larger TAs are present. These larger TAs are easily visible at the light microscope level, where they form long, spindle-shaped islands lacking cross striations and running for long lengths in the fiber (Fig. 3a). In sections for EM, the larger TAs clearly show multiple sub-clusters of tubules, with the semicrystalline axis of symmetry at varying orientations (Fig. 3b and c). This suggests that the large TAs are formed by coalescence of smaller individual TAs that were initiated by stochastic aggregation of tubules around independent crystallization centers. The dilated SR and/or irregular tubules that were present at the periphery of each individual TA (Fig. 2b) are trapped within the larger structures, appearing to surround each subcomponent (Fig. 3c, empty arrow). The center of each subcomponent is composed by rigidly cylindrical tubules as shown by freeze-fracture replicas (Fig. 3d and e).

Table 2 Relative surface areas and volumes of free SR in the I band and in TAs of type IIX–IIB fibers

Age	Sex	A Free SR V/V $\mu m^3/\mu m^3$	B Free SR Surface/V $\mu m^2/\mu m^3$	C Calculated V/V in TA centre[a] $\mu m^3/\mu m^3$	D Calculated S/V in TA centre[a] $\mu m^2/\mu m^3$
2–3 months	Male	0.08±0.02	6.4±1.4	–	–
7–8 months	Male	0.09±0.02	5.7±1.0	–	–
12 months	Male	0.10±0.04	5.2±1.0	–	–
24–29 months	Male	–	–	0.52	31.3

Mean±SD. Morphometric data are from five fibers each in three male mice

[a] Calculated on the basis of an average tubule diameter of 67 nm and an average tubule center to center distance of 82 nm

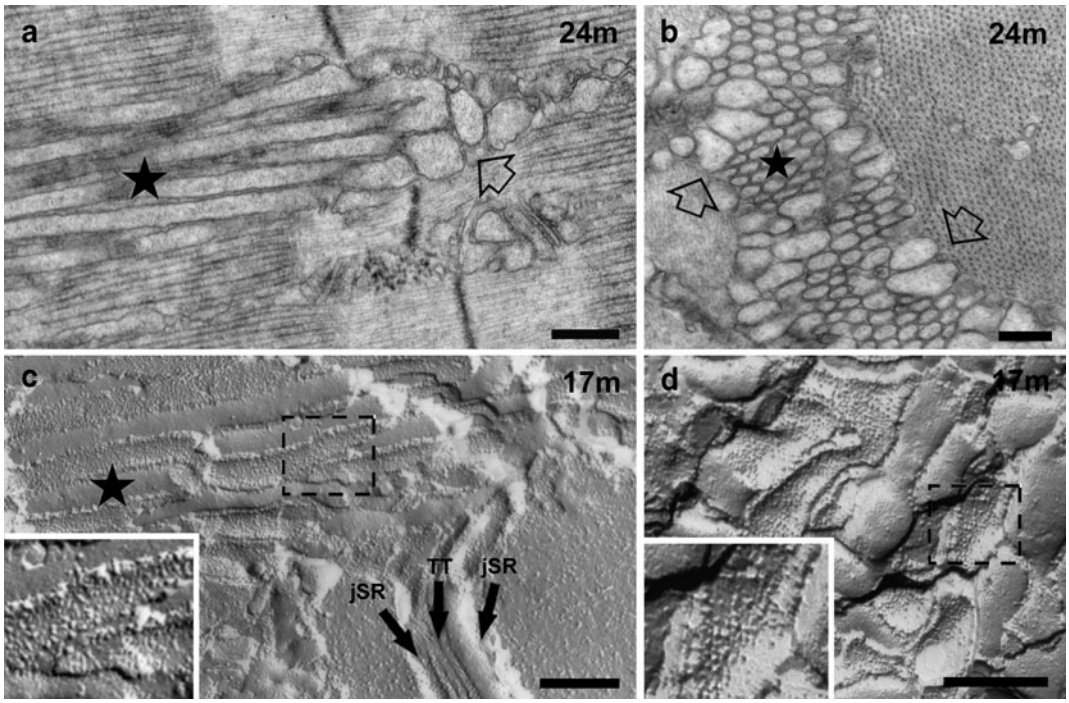

Fig. 2 The second step in the formation of TAs is the elongation and aggregation of parallel SR tubules, which protrude from the I into the A band. **a** The dilated SR tubules at the I band (*empty arrow*) elongate with age into longitudinal tubules that aggregate into parallel bundles (nascent TA, *star*). These bundles of tubules invade intermyofibrillar spaces at all levels of the sarcomere. **b** TAs are constituted of a peripheral ring of dilated SR profiles and irregularly shaped tubules (*empty arrows*) surrounding a central core of uniformly sized and regularly spaced tubules (*star*). **c**, **d** Parallel stacks of tubules growing from the I band into the A band are also visible in FF replicas (nascent TA, *star* in **c**). TA tubules (**c**) and dilated SR at the I band (**d**) are both uniformly covered by particles representing SERCA (*dashed boxes*). *Bars* 0.25 μm

SR–SR bridges connect regularly arranged SR tubules in TAs. The disposition and size of tubules at the center of TAs is sufficiently regular (Fig. 4a) that an electron optical diffraction pattern of their cross section gives reflections up to five orders (Fig. 4b). However, the spacing of the hexagonal pattern is not determined by the tubule diameter, because the tubules are not really touching each other but are separated by a relatively large distance (~6 nm membrane to membrane, Fig. 4a and c). The gap between adjacent tubules in TAs is crossed by discrete, evenly spaced bridges that directly connect tubules to adjacent neighbors (Fig. 4a and c, small arrows). Similar bridging structures have been also described in human TAs of patients suffering from TA myopathy (Chevessier et al. 2005) and are only occasionally present in normal SR, where some flat cisternae are closely apposed (not shown). The nature of the SR–SR bridges is unknown, but SERCA can be excluded as a candidate, because the bridges appear as discrete elements, while the headpieces of SERCA form a continuous halo around the SR (Wang et al. 1979; Campbell et al. 1980). The dense content of the cylindrical tubules in the core of TAs also acquires a very organized disposition often appearing as small circles parallel to the SR membrane (Fig. 4a).

Sarco(endo)plasmic reticulum Ca^{2+}-ATPase pumps (SERCA) is present at a high density in the tubular SR membrane of TAs and tends to acquire a spiral arrangement. SERCA is present in the free SR membrane of skeletal muscle, where the molecules are usually present at the maximum possible density. SERCA molecules are detectable as densely packed "particles" constituted of two to three molecules in FF replicas of the SR and as dots representing individual head pieces in rotary shadowed replicas of isolated SR vesicles (Franzini-Armstrong and Ferguson 1985). If the density of ATPase in the membrane is less than maximal, protein-free lipid patches appear (Ferguson et al. 1985). In EDL fibers at 17 months the

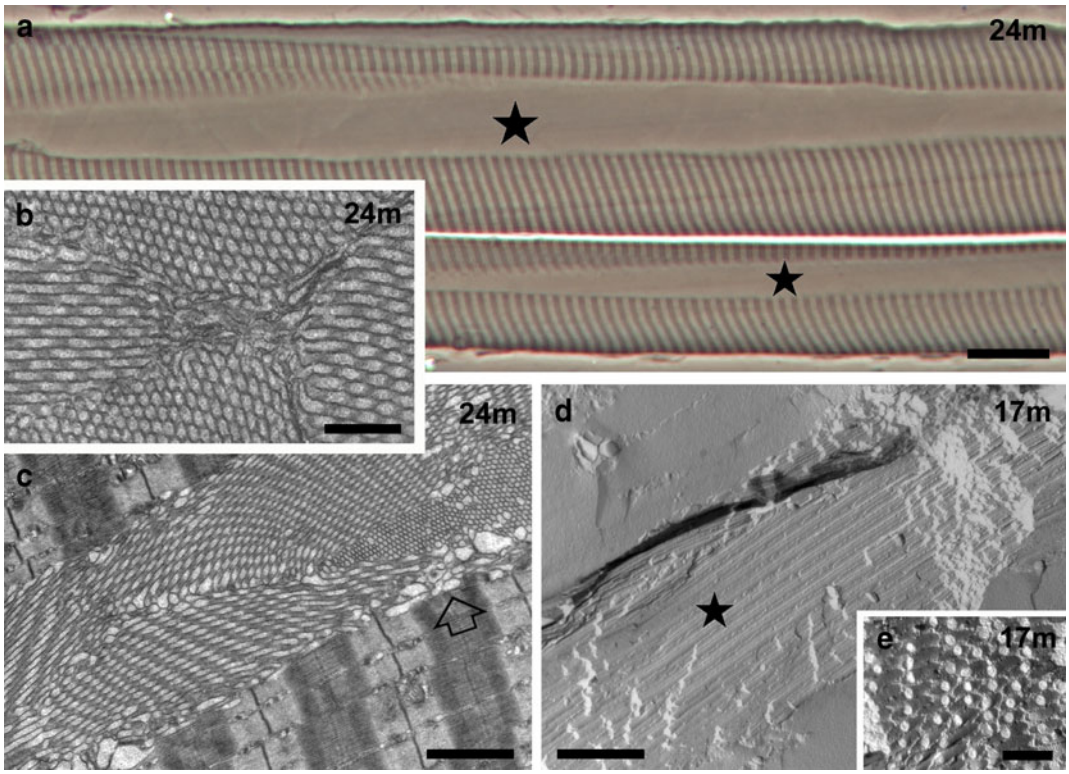

Fig. 3 TAs become larger and more frequent with age. **a** Phase contrast image showing two elongated striation free islands marking the position of TAs (*stars*). **b**, **c** Large TAs result from close association of multiple TAs, each with its ring of wider, more irregular tubules (**c**, *empty arrow*) and a central core of parallel and uniformly sized tubules. **d**, **e** The perfectly regular and straight shape of the core tubules is emphasized by freeze fracture replicas, where they appear as regular cylinders (**d**, *star*). The tubules transversely fractured in **e** displaying regular diameters. *Bars* **a** 20 μm; **b** 0.5 μm; **c** 2 μm; **d** 1 μm; **e** 0.25 μm

cytoplasmic leaflet of SR shows a uniform tight arrangement of particles over normal, dilated, and tubular SR indicating that the maximum complement of ATPase is maintained in all these membranes (Fig. 2c and d, dashed boxes, and Fig. 4d). In the membranes of cylindrical SR tubules within TAs, in addition, there is an unusual tendency towards a spiraling arrangement of the particles (Fig. 4f, arrows), which is better visible in some tubules than in others. Unusual elongated SR tubules are present in crude SR fractions from muscle at 17 months (Fig. 4g) but are absent in homogenates of muscles from younger animals (Paolini et al. 2004), allowing the identification of the elongated tubules as TAs' components. On the surface of some elongated tubules, the spiraling arrangement of SERCA tails is clearly detectable (Fig. 4g, arrows). This disposition is reminiscent of the semicrytalline array of SERCA in the membranes of tubular SR induced by vanadate (Ferguson et al. 1985).

CASQ is an integral component of TAs, but RYRs are rarely trapped into the aggregates. Immunolabeling for CASQ shows positive foci aligned along doublets of transverse rows corresponding to the location of triads and a diffuse labeling of the elongated, spindle-shaped TAs (Fig. 5a). Immunolabeling for RYRs also marks the double rows of triads, but the interior of TAs is mostly negative for this protein (Fig. 5b). However, RYR-positive spots stronger than those marking the triads between the myofibrils are abundant at the edges of the spindle-shaped TAs (Fig. 5c and d, arrows). Electron microscopy images confirm that triads are mostly outside the TAs but show an occasional accumulation of multiple T–SR stacks at the periphery, presumably responsible for the intense RYR foci (Fig. 5e, empty arrows). A few triads remain trapped inside the aggregate (Fig. 5g), thus providing an explanation for the rare presence of RYR-positive foci inside TAs (Fig. 5b, arrow). Trapping of mitochondria and T-tubules within TAs is also very rare (Fig. 5h and i).

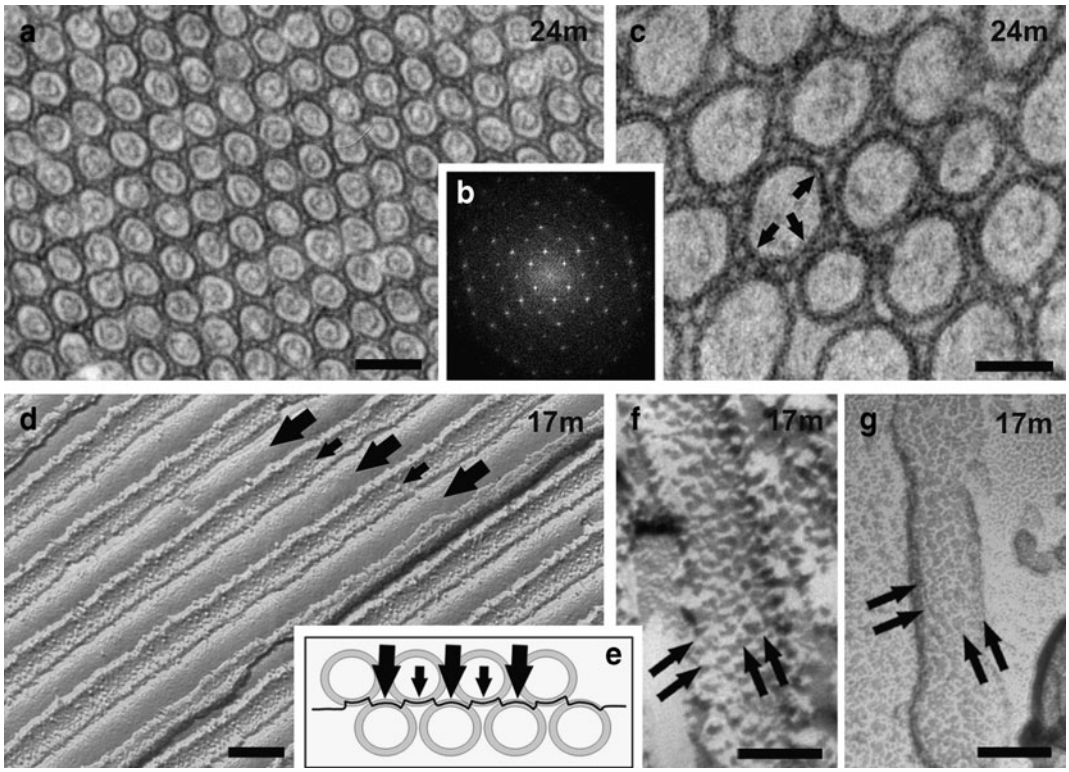

Fig. 4 In the core of large TAs, SR tubules are regularly arranged, perfectly cylindrical, covered by SERCA particles, and held together by little bridges. **a**, **b** Tubules in the center of TAs are arranged in a highly ordered hexagonal pattern (**a**), giving rise to an electron optical diffraction transform that indexes on 60° angles and shows up to five orders of reflections (**b**). **c** The ordered arrangements of tubules is probably maintained, if not established, by frequent cross links of uniform size that bridge the gap between the membrane of adjacent tubules (*small arrows*). **d** Tubules in the center of large TAs are perfectly straight resulting—when freeze-fractured and replicated—in regularly alternated views of the luminal and cytoplasmic (*large and small arrows*, respectively) leaflets. **e** A diagram modeling the plane of fracture that exposes alternatively luminal and cytoplasmic leaflets of the tubules (*large and small arrows*, respectively). **f** The cytoplasmic leaflet is decorated by particles representing small aggregates of SERCA molecules. The particles show tendency towards a helical arrangement (**f**, *arrows*), which is best detected by holding the image at eye level and glancing along the direction of the two sets of *arrows*. **g** A more precise view of the helical symmetry of SERCA particles (*arrows*) is visible on the free cytoplasmic surface of an SR tubule isolated from aging muscle and prepared by freeze-drying, rotary shadowing. *Bars* **a**, **d** 0.1 μm; **b**, **e**, **g** 0.05 μm

SR aggregates are present in CASQ null muscle, but they are smaller and structurally different from TAs. Type IIB–IIX fibers of EDL from CASQ1-null mice develop modest aggregates of tubules which share with TAs an SR origin but are structurally different and also have a different distribution and age dependence. The CASQ-null aggregates appear at young ages (as early as 4 months), in both males and females, and usually do not progress beyond small dimensions (at most, ~10–15 μm in length and ~1–2 in width, Fig. 6a and d, star). Like TAs, these aggregates are composed of multiple, tightly aggregated tubules of fairly uniform diameter, clearly continuous with the SR (Fig. 6b). However, unlike those of TAs, the CASQ-null tubules do not become straight and follow a tortuous path. The junctional SR cisternae in these fibers seem to be periodically pinched (Fig. 6b, arrowheads), showing a scalloped outline and well visible electron-dense dots in the lumen (Fig. 6b). The dots are clearly not composed of CASQ1, a protein that is totally absent in these fibers (Paolini et al. 2007). The SR aggregates in CASQ1-null fibers seem to be a repetition of this structure in the sense that small dense dots are present inside each circular sectioned tubule profile and that the size of the circles is similar to the scallops in the jSR. Thus, it is conceivable that the aggregate form from replication/proliferation of the jSR cisternae. Higher magnification of the core of an aggregate

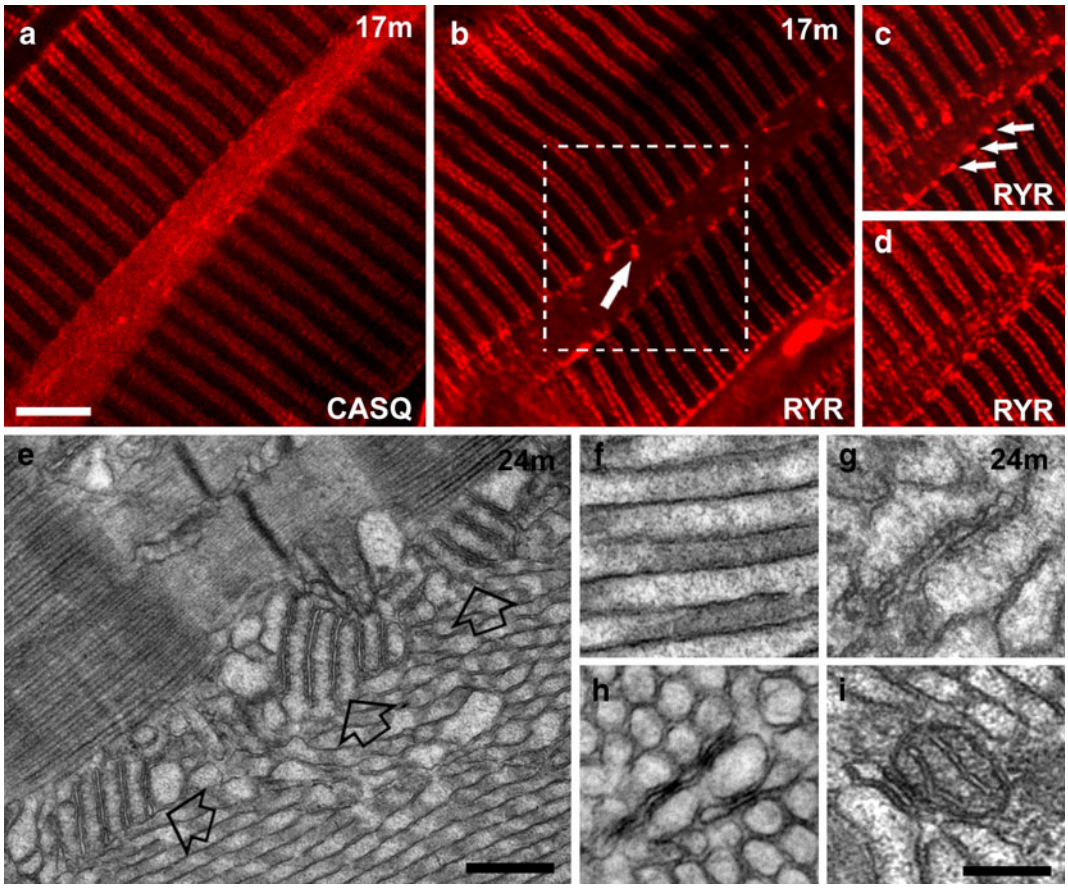

Fig. 5 TAs contain CASQ, but not RyRs. Mitochondria, T-tubules, and triads are only occasionally trapped within the aggregate. **a**, **b** Immunostaining of EDL fibers with antibodies against CASQ and RYR reveals that TAs contain CASQ (**a**, see also **f**), but not RYR (**b**). Bright RYR-positive spots (*arrow* in **b**), representing trapped triads (see also **g**), are rare. **c**, **d** Two different optical sections of the area marked in **b** by the *dashed box* show RYR positive spots at the edges of a optically sectioned TA (**c**, *arrows*; see also **e**) and in a plane grazing the TA (**d**). **e** Stacks of SR-T-tubules junctions (*empty arrows*) containing RYRs are frequently present at the TA's edge (compare with **c**). **f** TAs' tubules are filled with electron-dense material, most likely CASQ. **g–i** SR/T-tubule junctions (or triads, **g**), T-tubules (**h**), and mitochondria (**i**) are rarely trapped inside TAs, mostly where smaller TAs merge with each other (see also Fig. 3b). *Bars* **a–d**, 5 μm; **e** 0.5 μm; **f–i** 0.2 μm

shows that tubules are not connected by SR–SR bridges in CASQ1 null EDL fibers (Fig. 6c). However, occasionally, small bridges are present where an unusual aggregation of two to three flat SR cisternae which partially surround the aggregate, are closely apposed to each other (Fig. 6c and inset).

Discussion

The presence of TAs in fast-twitch muscle fibers at late ages (Agbulut et al. 2000) and their precocious formation in senescence-accelerated mice (Nishikawa et al. 2000) have suggested that these structures are a peculiar expression of aging. In this work, we show, however, that TAs are not simply the result of events set in motion late in life, but instead, they represent the final stage in a slow and progressive SR modification that start quite early after the initial SR differentiation is complete, but surprisingly quite early, and that involves several sequential steps. Thus, TAs' formation is age dependent simply because it begins only after large amounts of extra CASQ have accumulated, and additional SERCA and membrane lipids are added. TAs' formation is also not directly related to senescence, because it starts quite early in some muscles (Agbulut et al.

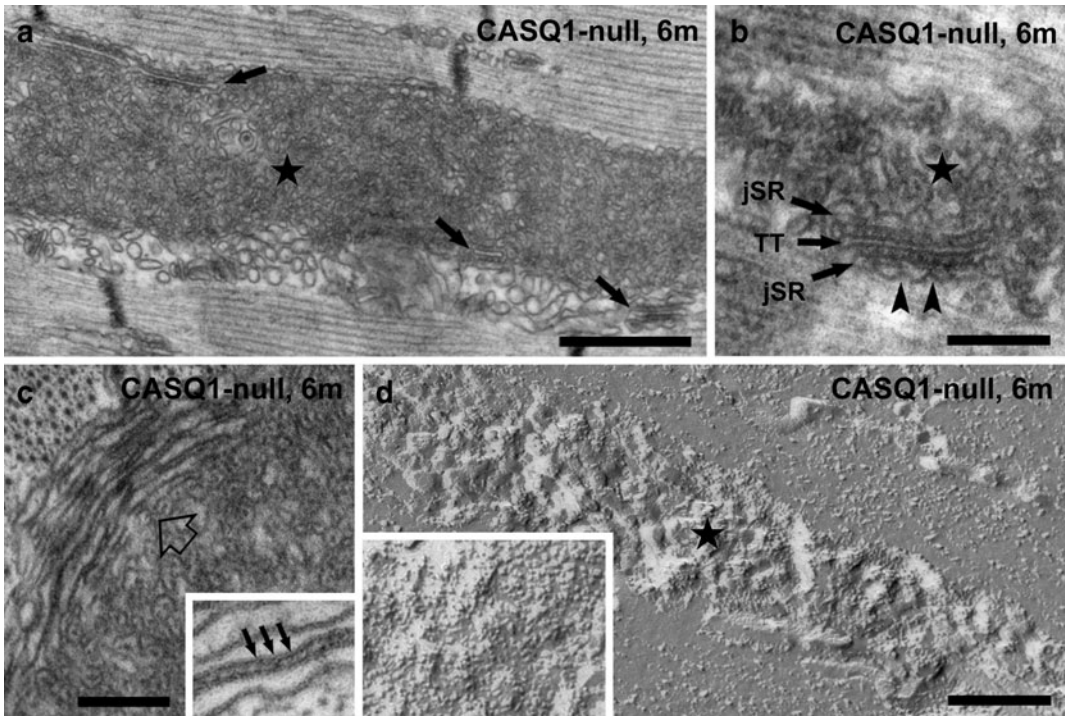

Fig. 6 Abnormal aggregates of SR tubules in CASQ1-null fibers are present, but they never became straight, cylinder shaped, and orderly. **a**, **b** CASQ1-null aggregates of SR tubules (**a**, *star*), continuous with the jSR of triads (**a**, **b**, *arrows*), are composed of tubules/sacs smaller in diameter that those described for TAs in WT fibers and remain convoluted. The jSR cisternae in these fibers are periodically pinched (**b**, *arrowheads*) and display a scalloped outline. **c** Characteristic stacks of flat SR cisternae (*empty arrow*) are occasionally present immediately next to SR aggregates. These stacks are tethered together by small bridges (detail in **c**, *small arrows*). **d** In freeze-fracture replicas, the CASQ1-null SR aggregates contain particles, presumably SERCA, in the cytoplasmic leaflet, which do not show any sign of helical symmetry (detail in **d**). *Bars* **a** 0.5 μm; **b**–**d** 0.2 μm

2000). In addition, here, we also show that lack of CASQ1 impairs TAs maturation into straight, parallel, and regularly sized tubules.

The timing and sequence of free SR changes in early adulthood provide a temporal framework for the events leading to formation of TAs and to their maturation in IIX–IIB fibers. Initially, the SR becomes dilated and shows an accumulation of electron-dense material (presumably CASQ, see below) in their lumen. This change affects specifically the junctional and free SR elements positioned at I-Z-I band domain, leaving the A band SR unaffected (Figs. 1 and 7). This dilation of the SR elements is not accompanied by an overall increase in volume and surface area (the latter actually marginally decreases with age) because while the SR tubules become larger in diameter, they also decrease in number, so that overall, the SR shape becomes less convoluted. Several lines of evidence support the conclusion that the electron-dense polymer that is visible in the widening SR tubules at the I band is indeed CASQ. First, a net accumulation CASQ has been directly demonstrated by western blotting in muscle presenting TAs (Chevessier et al. 2004). Second, experimental overexpression of CASQ2 and CASQ1, respectively, in cardiac (Tijskens et al. 2003; Sato et al. 1998) and skeletal (Tomasi et al. 2009) muscle, results in swelling of the SR, which appear filled by an electron dense polymer. The initial accumulation of CASQ in I band SR is likely not a direct cause of TAs' formation, since CASQ accumulation occurs in both male and female mice (Chevessier et al. 2004), but TAs are present only in the former and overexpression of CASQ (see references above) does not lead to TA formation. Additionally, SR dilation never occurs (even at late ages) in fibers from CASQ1-null mice (Paolini et al. 2007), indicating that this phenomenon may be driven by CASQ type-1 in EDL (Figs. 1, 6, 7). Finally, CASQ accumulation in TAs is

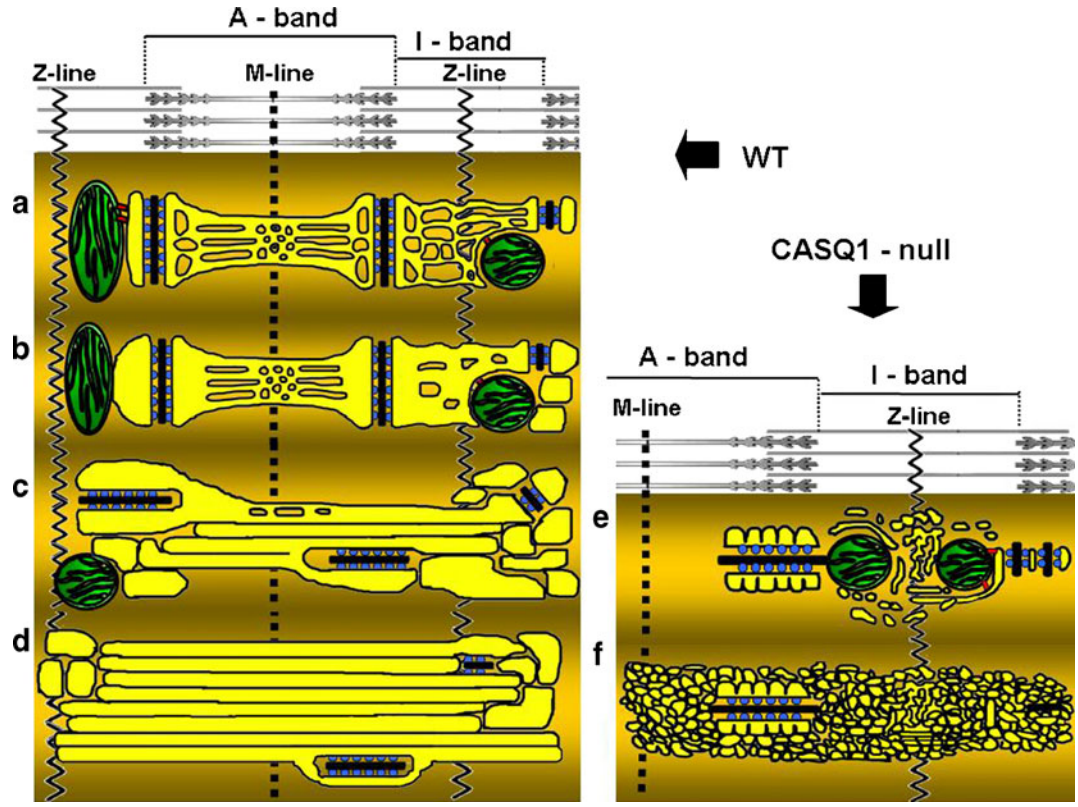

Fig. 7 Modeling of **a**–**d** sequential steps leading to formation of TAs in WT fast glycolytic fibers; **e**, **f** impaired assembly of TAs in CASQ1-null fibers. **a** Normal morphology of SR and triads in adult fibers. In adult mammalian muscle, the SR (*yellow*) is comprised of two domains: (1) jSR constituting the two lateral sacs of a triads, comprising two arrays of RYRs (*blue*); and (2) free SR, that extends on both sides of the triad, along the entire sarcomere. The T tubule is in black. The I band free SR is composed mostly of irregular and convoluted tubules, whereas the A band free SR is a combination of tubules and flat fenestrated cisternae (see Fig. 1). **b** Dilatation of I band SR. Around 12 months of age, junctional and free SR at the I band level of fast twitch fibers in males is often abnormally dilated, whereas A band free SR maintains its usual shape (see Fig. 1). **c** Elongation of tubules into the A band. With increasing age (17–24 months) the dilated junctional and free I band SR projects elongated, cylindrical longitudinal tubules. Triads become more frequently longitudinal (see Fig. 2). **d** Formation of large tubular aggregates. Growing accumulation of tubules becomes TAs that displace all other cell organelles and coalesce into increasingly larger aggregates. Dilated SR cisternae and triads are mostly confined to the TAs edges (see Figs. 3 and 5). **e**, **f** TAs do not develop without CASQ1. In CASQ1-null fibers the jSR cisternae width is significantly reduced compared to the WT (Paolini et al. 2007). The membrane of jSR cisternae displays a scalloped profile on the side opposite to the T-tubule.CASQ1-null SR tubules at the I band level remains narrow and very convoluted, even where they occasionally accumulate into aggregates reminiscent of but not identical to TAs

directly demonstrated at later stages by positive immunolabeling of TAs with anti-CASQ1 antibodies (Fig. 5). An interesting observation is that the initial accumulation of CASQ is specifically restricted to the I band level SR. The extra CASQ spills into the A band SR only rarely in normal mice, although more frequently under some pathological conditions (Boncompagni et al. 2010). Thus, even though the TAs' SR tubules run for long distances longitudinally, the adjacent A band level free SR is not affected. The differential response of the two SR domains indicates that the I band SR has some distinctive properties, even though it is directly connected to the SR covering the A band by extensions that bypass the triads. Indeed, triadin isoforms, Trisk 49 and 32, are differentially distributed over the I-Z-I region (Vassilopoulos et al. 2005) and the absence of obscurin, a presumed component of the SR-myofibrils link, affects the A band SR, but not the I band SR (Lange et al. 2009).

A second distinct series of events, requiring new yet undefined mechanisms, starts at ~15 months of age in EDL but at earlier ages in other muscles

(Agbulut et al. 2000), with the formation and accumulation of elongated SR tubules, followed by their segregation into ordered, but still fairly small, TAs (Figs. 2 and 7). Several months separate the early SR dilation and the first formation of TAs. A specific increase in SERCA and CASQ content of aged muscles containing TAs has been demonstrated by western blotting (Chevessier et al. 2004). We estimate that the surface density and the relative volume of SR tubules within TAs are, respectively, ~6- and 5-fold higher than those of the I band SR (Table 1). Since SR surface in TAs is fully decorated by SERCA molecules (Fig. 4) and the lumen contains CASQ (Fig. 5), we predict that SERCA and CASQ content in TAs must be higher than in the I band SR. TAs grow in size at a slow rate, over a period of several months. At this stage, we cannot exclude the possibility that the accumulation of membranes and proteins in TAs is due to a rearrangement of the SR elements normally present between the myofibrils, rather than to de novo growth. In this respect, slow and age-dependent formation of TAs likely differs significantly from the mechanism leading to TAs' formation during ischemic challenges (Schiaffino et al. 1977), which involves a rapid (few hours) redistribution of existing SR elements.

The progressive transformation of SR tubules into rigid cylinders of fairly constant diameter as they become trapped in the TAs cores requires a mechanism that seems to be absent in CASQ1-null fibers where SR' tubules remain wavy and irregular (Figs. 6 and 7). One hint comes from the observation that mature TA tubules display a specific, although not always perfect, semicrystalline, helical arrangement of SERCA in their membrane (Fig. 4). This disposition and the tubular shape of the SR closely mimic that of elongated SR tubules bearing two-dimensional SERCA crystals that result from block of SERCA into an inactive configuration by exposure to vanadate (Dux and Martonosi 1983). Similarly, crystallization of SERCA, both within the membrane or extracted from it, strictly requires immobilization of the molecule into one of several states in the reaction cycle (Toyoshima et al. 2004). The inferences from these observations are that polymerization of SERCA into a semicrystalline arrangement is the mechanism that induces the core tubules of TAs to become straight and that SERCA in the central TAs' tubules may become gradually inactive. The specific cause of the SERCA inactivation is not known, but a good possibility is that it simply results from the segregation of excessive SERCA into fiber domains where it is not exposed to cyclic changes in Ca^{2+} concentrations. Such an event has been actually experimentally mimicked by exposing skinned muscle fibers to a constant low Ca^{2+} level (Castellani et al. 1989), an experiment which cannot unfortunately be carried on in vivo. The slow increase in TAs' size with age is likely driven by the accrual of elements from the persistent peripheral rim of dilated SR profiles (Fig. 2). Further growth is due to aggregation of independently generated TAs in to larger one, which displays domains of tubules with multiple orientations (Fig. 3).

Several points remain unclear in this apparently logical sequence of events. Although apparently there is no direct connection between CASQ accumulation in I band SR and the subsequent formation of TAs, indirect evidence points to a possible link between the two events: (1) in WT females, CASQ accumulation and related SR dilation are very limited and the elongation of tubules is never observed (not shown); (2) tubules appear to elongate from I-band dilated SR and not from the A-band SR, which is not dilated (Figs. 2 and 7); (3) in knockout fibers CASQ accumulation cannot occur and regular TAs are not formed (Figs. 1, 6, 7); (4) dilated SR seems to be the source of tubule accrual during the growth of TAs (Fig. 2). This said, mechanisms leading to TAs' formation and maintenance deserves further investigation. SERCA crystallization can in itself be a driving force toward tubular elongation. Data in literature suggest that this event may not require CASQ, because it can be induced in isolated "light" SR vesicles that likely do not contain CASQ (Dux and Martonosi 1983). However, CASQ may contribute to determine size and stability of the cylindrical tubules, since elongated SR tubules form in CASQ-null fibers, but the tubules remain highly convoluted and never transition to a straight cylindrical shape (Figs. 6 and 7). A second element that is likely fundamental to stabilize TAs is the yet unidentified protein that forms regular bridges connecting TAs' tubules to each other (Fig. 4). Such bridges are not observed in the less stable SR aggregates of CASQ-null mice.

As an explanation for the accumulation of SR proteins involved in Ca^{2+} uptake and storage (Chevessier et al. 2004; Salviati et al. 1985), it has been suggested that TAs may arise in response to a requirement for extra Ca^{2+} uptake in order to prevent muscle fibers from hypercontraction and necrosis (Muller et al. 2001; Salviati et al. 1985; Schubert et al. 2007). However, even though resting cytoplasmic Ca^{2+} levels are slightly elevated in old-aged rat muscle (Fraysse et al. 2006), we note that the events leading to TAs' formation start at an early age, and they are restricted to the more glycolytic fast fibers, which have more limited pattern of activity. Additionally, TAs segregate CASQ and SERCA away from the myofibrils and contain SERCA that is likely blocked in a nonfunctional configuration. Based on our observations, we propose the alternate hypothesis that TAs do not participate actively in the fibers' Ca^{2+} homeostasis but may simply act as deposit sites for accumulated proteins.

Acknowledgements We thank Drs. Osvaldo Delbono and Cecilia Paolini for providing samples of aged female mice and CASQ1 null mice used in this study. We thank L. R. Jones (Indiana University) for the generous gift of anti CASQ antibody 4B1.D3. This study was supported by National Institutes of Health Grant 5P01AR052354 to C.F.A. and by Telethon Research Grant GGP08153 to F.P.

References

Agbulut O, Destombes J, Thiesson D, Butler-Browne G (2000) Age-related appearance of tubular aggregates in the skeletal muscle of almost all male inbred mice. Histochem Cell Biol 114(6):477–481

Airey JA, Beck CF, Murakami K, Tanksley SJ, Deerinck TJ, Ellisman MH, Sutko JL (1990) Identification and localization of two triad junctional foot protein isoforms in mature avian fast-twitch skeletal muscle. J Biol Chem 265:14187–14194

Augusto V, Padovani CR, Campos GER (2004) Skeletal muscle fiber types in c57bl6j mice. Braz J morphol Sci 21(2):89–94

Boncompagni S, d'Amelio L, Fulle S, Fano G, Protasi F (2006) Progressive disorganization of the excitation-contraction coupling apparatus in aging human skeletal muscle as revealed by electron microscopy: A possible role in the decline of muscle performance. J Gerontol A Biol Sci Med Sci 61(10):995–1008

Boncompagni S, Loy RE, Dirksen RT, Franzini-Armstrong C (2010) The I4895T mutation in the type 1 ryanodine receptor induces fiber-type specific alterations in skeletal muscle that mimic premature aging. Aging Cell 9(6):958–970

Campbell KP, Franzini-Armstrong C, Shamoo AE (1980) Further characterization of light and heavy sarcoplasmic reticulum vesicles. Identification of the 'sarcoplasmic reticulum feet' associated with heavy sarcoplasmic reticulum vesicles. Biochim Biophys Acta 602(1):97–116

Castellani L, Hardwicke PM, Franzini-Armstrong C (1989) Effect of ca2+ on the dimeric structure of scallop sarcoplasmic reticulum. J Cell Biol 108(2):511–520

Chevessier F, Marty I, Paturneau-Jouas M, Hantai D, Verdiere-Sahuque M (2004) Tubular aggregates are from whole sarcoplasmic reticulum origin: Alterations in calcium binding protein expression in mouse skeletal muscle during aging. Neuromuscul Disord 14(3):208–216

Chevessier F, Bauché-Godard S, Leroy JP, Koenig J, Paturneau-Jouas M, Eymard B, Hantaï D, Verdière-Sahuqué M (2005) The origin of tubular aggregates in human myopathies. J Pathol 207(3):313–323

Craig ID, Allen IV (1980) Tubular aggregates in murine dystrophy heterozygotes. Muscle Nerve 3(2):134–140

D'Incecco A, Dainese M, Protasi F, Boncompagni S (2010) Progressive triad-mitochondria un-coupling in aging. Biophys J 98:A547

Danieli-Betto D, Esposito A, Germinario E, Sandona D, Martinello T, Jakubiec-Puka A, Biral D, Betto R (2005) Deficiency of alpha-sarcoglycan differently affects fast- and slow-twitch skeletal muscles. Am J Physiol Regul Integr Comp Physiol 289(5):R1328–1337

Dux L, Martonosi A (1983) The regulation of atpase-atpase interactions in sarcoplasmic reticulum membrane. Ii. The influence of membrane potential. J Biol Chem 258 (19):11903–11907

Engel WK (1964) Mitochondrial aggregates in muscle disease. J Histochem Cytochem 12:46–48

Engel WK, Bishop DW, Cunningham GG (1970) Tubular aggregates in type ii muscle fibers: Ultrastructural and histochemical correlation. J Ultrastruct Res 31(5–6):507–525

Ferguson DG, Franzini-Armstrong C, Castellani L, Hardwicke PM, Kenney LJ (1985) Ordered arrays of ca2+-atpase on the cytoplasmic surface of isolated sarcoplasmic reticulum. Biophys J 48(4):597–605

Franzini-Armstrong C, Ferguson DG (1985) Density and disposition of ca2+-atpase in sarcoplasmic reticulum membrane as determined by shadowing techniques. Biophys J 48(4):607–615

Fraysse B, Desaphy JF, Rolland JF, Pierno S, Liantonio A, Giannuzzi V, Camerino C, Didonna MP, Cocchi D, De Luca A, Conte Camerino D (2006) Fiber type-related changes in rat skeletal muscle calcium homeostasis during aging and restoration by growth hormone. Neurobiol Dis 21(2):372–380

Hughes SM, Chi MM, Lowry OH, Gundersen K (1999) Myogenin induces a shift of enzyme activity from glycolytic to oxidative metabolism in muscles of transgenic mice. J Cell Biol 145(3):633–642

Jones LR, Suzuki YJ, Wang W, Kobayashi YM, Ramesh V, Franzini-Armstrong C, Cleemann L, Morad M (1998) Regulation of Ca2_ signaling in transgenic mouse cardiac myocytes overexpressing calsequestrin. J Clin Invest 101:1385–1393.

Lange S, Ouyang K, Meyer G, Cui L, Cheng H, Lieber RL, Chen J (2009) Obscurin determines the architecture of the

longitudinal sarcoplasmic reticulum. J Cell Sci 122(Pt 15):2640–2650

Meissner G, Conner GE, Fleischer S (1973) Isolation of sarcoplasmic reticulum by zonal centrifugation and purification of ca 2+ -pump and ca 2+ -binding proteins. Biochim Biophys Acta 298(2):246–269

Morgan-Hughes JA (1998) Tubular aggregates in skeletal muscle: Their functional significance and mechanisms of pathogenesis. Curr Opin Neurol 11(5):439–442

Muller HD, Vielhaber S, Brunn A, Schroder JM (2001) Dominantly inherited myopathy with novel tubular aggregates containing 1–21 tubulofilamentous structures. Acta Neuropathol 102(1):27–35

Niakan E, Harati Y, Danon MJ (1985) Tubular aggregates: Their association with myalgia. J Neurol Neurosurg Psychiatry 48(9):882–886

Nishikawa T, Takahashi JA, Matsushita T, Ohnishi K, Higuchi K, Hashimoto N, Hosokawa M (2000) Tubular aggregates in the skeletal muscle of the senescence-accelerated mouse; sam. Mech Ageing Dev 114(2):89–99

Novotova M, Zahradnik I, Brochier G, Pavlovicova M, Bigard X, Ventura-Clapier R (2002) Joint participation of mitochondria and sarcoplasmic reticulum in the formation of tubular aggregates in gastrocnemius muscle of ck-/- mice. Eur J Cell Biol 81(2):101–106

Paolini C, Protasi F, Franzini-Armstrong C (2004) The relative position of ryr feet and dhpr tetrads in skeletal muscle. J Mol Biol 342(1):145–153

Paolini C, Quarta M, Nori A, Boncompagni S, Canato M, Volpe P, Allen PD, Reggiani C, Protasi F (2007) Reorganized stores and impaired calcium handling in skeletal muscle of mice lacking calsequestrin-1. J Physiol 583(Pt 2):767–784

Pavlovicova M, Novotova M, Zahradnik I (2003) Structure and composition of tubular aggregates of skeletal muscle fibres. Gen Physiol Biophys 22(4):425–440

Pierobon-Bormioli S, Armani M, Ringel SP, Angelini C, Vergani L, Betto R, Salviati G (1985) Familial neuromuscular disease with tubular aggregates. Muscle Nerve 8(4):291–298

Rosenberg NL, Neville HE, Ringel SP (1985) Tubular aggregates. Their association with neuromuscular diseases, including the syndrome of myalgias/cramps. Arch Neurol 42(10):973–976

Salviati G, Pierobon-Bormioli S, Betto R, Damiani E, Angelini C, Ringel SP, Salvatori S, Margreth A (1985) Tubular aggregates: sarcoplasmic reticulum origin, calcium storage ability, and functional implications. Muscle Nerve 8 (4):299–306

Sato Y, Ferguson DG, Sako H, Dorn GW 2nd, Kadambi VJ, Yatani A, Hoit BD, Walsh RA, Kranias EG (1998) Cardiac-specific overexpression of mouse cardiac calsequestrin is associated with depressed cardiovascular function and hypertrophy in transgenic mice. J Biol Chem 273(43):28470–28477

Schiaffino S, Severin E, Cantini M, Sartore S (1977) Tubular aggregates induced by anoxia in isolated rat skeletal muscle. Lab Invest 37(3):223–228

Schubert W, Sotgia F, Cohen AW, Capozza F, Bonuccelli G, Bruno C, Minetti C, Bonilla E, Dimauro S, Lisanti MP (2007) Caveolin-1(-/-)- and caveolin-2(-/-)-deficient mice both display numerous skeletal muscle abnormalities, with tubular aggregate formation. Am J Pathol 170(1): 316–333

Tijskens P, Jones LR, Franzini-Armstrong C (2003) Junctin and calsequestrin overexpression in cardiac muscle: The role of junctin and the synthetic and delivery pathways for the two proteins. J Mol Cell Cardiol 35(8):961–974

Tomasi M, Canato M, Paolini C, Dainese M, Reggiani C, Protasi F, Volpe P, Nori A (2009) Expression of calsequestrin-1 (cs1) in cs1-null mice: restoration of calcium release unit architecture and amplitude of calcium transient in fast-twitch muscle fibers. Biophys J 96 (3):236a–237a

Toyoshima C, Nomura H, Tsuda T (2004) Lumenal gating mechanism revealed in calcium pump crystal structures with phosphate analogues. Nature 432(7015):361–368

Vassilopoulos S, Thevenon D, Rezgui SS, Brocard J, Chapel A, Lacampagne A, Lunardi J, Dewaard M, Marty I (2005) Triadins are not triad-specific proteins: Two new skeletal muscle triadins possibly involved in the architecture of sarcoplasmic reticulum. J Biol Chem 280(31):28601–28609

Vielhaber S, Schroder R, Winkler K, Weis S, Sailer M, Feistner H, Heinze HJ, Schroder JM, Kunz WS (2001) Defective mitochondrial oxidative phosphorylation in myopathies with tubular aggregates originating from sarcoplasmic reticulum. J Neuropathol Exp Neurol 60(11):1032–1040

Wang CT, Saito A, Fleischer S (1979) Correlation of ultrastructure of reconstituted sarcoplasmic reticulum membrane vesicles with variation in phospholipid to protein ratio. J Biol Chem 254(18):9209–9219

Yoshitoshi M, Ishihara T, Yoshimura Y, Tsugane T, Shinohara Y (1991) the effect of sex hormones on tubular aggregates in normal mouse skeletal muscles. Rinsho Shinkeigaku 31 (9):974–980